$K_{10}In_{10}Z$ (Z = Ni, Pd, or Pt): Zintl Phases Containing Isolated Decaindium Clusters Centered by Transition Elements

Slavi C. Sevov and John D. Corbett*

Contribution from the Department of Chemistry and Ames Laboratory—DOE,[1] Iowa State University, Ames, Iowa 50011

Received April 26, 1993®

Abstract: The isostructural title compounds are obtained by high yield by slowly cooling the appropriate fused mixture in welded Ta. They occur in the orthorhombic space group *Pnma*, $Z = 12$, with $a = 15.948(6)$, 16.043(6), 16.056(3) Å, $b = 32.565(6)$, 32.73(1), 32.692(1) Å, and $c = 18.822(3)$, 18.895(5), 18.896(3) Å for the Ni, Pd, and Pt derivatives, respectively. The structure of the Ni phase was refined by single crystal means (R, R_w = 2.9, 3.3%) and shown to be constructed from close-packed layers of Ni-centered In_{10} clusters that are separated by potassium ions both within and between the cluster layers. The compounds have large resistivities at room temperature by two-probe methods and are diamagnetic, with no moments on the transition metals. The geometry of the clusters can be derived from an ideal tetracapped trigonal prism (C_{3v}) of In centered by Z through axial compression along the 3-fold axis and opening of the capped triangular face so as to yield substantially equal Ni–In distances. The clusters are also related to Sb_7^{3-}, etc. Charge-consistent extended-Hückel MO calculations show that the Ni-centered cluster has a closed shell with $2n = 20$ skeletal electrons, only the s and p orbitals on the interstitial mixing with appropriate cluster orbitals. The d orbitals on Ni do not appear to participate significantly, presumably because they are fully reduced (lie too low) relative to In p (d(In–Ni) ~ 2.8 Å). This means that Ni, Pd, and Pt behave as quasi-main-group elements.

Introduction

Although indium lies three periods below boron, its ability to form a variety of isolated clusters with homoatomic covalent bonding parallels that of the familiar boranes $B_nH_n^{2-}$ surprisingly well. Of course, indium analogues with exo-bonded H, R, etc. are not stable, but alternative "naked" clusters are. However, a potential problem remains with such clusters, the apparent requirement of at least $2n + 2$ skeletal electrons for closo-polyhedra (Wade's rules) that is repeatedly observed with boranes, carboranes, etc.[2] or in analogues with later, heavier elements like Sn_9^{4-}, Pb_5^{2-}, and so forth (Zintl ions).[3] This minimum would require that closo clusters of n In atoms have unusually high charges, especially when n is large, viz. $In_n^{(n+2)-}$. Indium generally avoids this circumstance by forming either clusters with new geometries that are hypoelectronic with respect to these rules[4] or borane-type clusters with several two-center exo bonds between them that reduce the charge on each cluster by one per bond.[5,6]

Small tetrahedral (nido) clusters, formally In_4^{8-}, are still found in Na_2In. The charge on the cluster is apparently not too high, and a common geometry is retained.[6] The situation is different in 10- and 11-atom indium clusters. The latter are represented by In_{11}^{7-} and the substitution product $In_{10}Hg^{8-}$ in K_8In_{11} and $K_8In_{10}Hg$, respectively.[4,7] Both clusters have a geometry unknown for boranes, a pentacapped trigonal prism compressed along the 3-fold axes that requires $2n$ - 4 skeletal electrons. A third type of cluster is the Zn-centered $In_{10}Zn^{8-}$ found in $K_8In_{10}Zn$.[8] Although this has a classical geometry, a bicapped Archemedian antiprism, it is distorted through compression along the 4-fold axis so that all Zn–In separations are about equal. This unit now requires $2n$ rather than $2n + 2$ skeletal bonding electrons, two of the former being provided by the zinc. This particular situation is in many respects quite similar to that in the many interstitially-stabilized cluster halides of the early transition metals.[9]

Gallium, in a great contrast with indium, has been reported to form alkali-metal compounds with structures consisting exclusively of cluster networks. Many binary and ternary alkali-metal–gallium–third element systems have been explored without finding any examples of isolated gallium clusters.[10] It is not yet clear whether such gallium analogues exist, but have been missed, or simply are not stable with respect to other compounds.

The discovery that indium clusters can be centered by zinc sparked a search for other elements that might act similarly in ternary alkali-metal–indium-third element systems. The compounds reported here were obtained directly from reactions designed to produce $K_{10}In_{10}Z$ (Z = Ni, Pd, or Pt) isoelectronic with $K_8In_{10}Zn$. In fact, Z-centered clusters in these have a different configuration and thus represent a fourth example of a family of relatively large, naked indium clusters.

Experimental Section

Mixtures of the elements (K, J. T. Baker, lump under oil, 98 + %; In, Cerac, shot, 99.999%; Ni, Matheson, Coleman & Bell, sheet, reagent grade; Pd, Johnson Mathey, wire, 99.995%; Pt, government issue, sheet, reagent grade) in atomic ratios K:In:(Ni, Pd, Pt) = 10:10:1 were fused in closed Ta containers at 600 °C for 2 days and then cooled slowly (3 deg/h) to room temperature. The melting points are about 480 °C. (The technique is described in more detail elsewhere.[6]) The products were in the form of loose bar- or gem-like crystallites with dull and dark yellowish appearances. They react rapidly with air, the condensed moisture producing hydrogen and boiling in a minute or two, and surface contamination from handling even within a Vacuum Atmospheres glovebox is sufficient to preclude useful XPS data. Other reactions loaded to produce analogous potassium or sodium compounds containing Sc, Ti, Cr, Mn, Fe, Co, Ru, or Rh yielded only known binary products according to their powder patterns.

® Abstract published in *Advance ACS Abstracts*, September 1, 1993.

(1) The Ames Laboratory is operated for the U.S. Department of Energy by Iowa State University under Contract No. W-7405-Eng-82. This research was supported by the Office of the Basic Energy Sciences, Materials Sciences Division, DOE.

(2) Greenwood, N. N.; Earnshaw, A. *Chemistry of the Elements*; Pergamon Press: Oxford, UK, 1984; pp 171–209.

(3) Corbett, J. D. *Chem. Rev.* **1985**, *85*, 383.

(4) Sevov, S. C.; Corbett, J. D. *Inorg. Chem.* **1991**, *30*, 4875.

(5) Sevov, S. C.; Corbett, J. D. *Inorg. Chem.* **1992**, *31*, 1895.

(6) Sevov, S. C.; Corbett, J. D. *J. Solid State Chem.* **1993**, *103*, 114.

(7) Sevov, S. C.; Ostenson, J. E.; Corbett J. D. *J. Alloys Comp.*, accepted for publication.

(8) Sevov, S. C.; Corbett, J. D. *Inorg. Chem.* **1993**, *32*, 1059.

(9) Ziebarth, R. P.; Corbett, J. D. *Acc. Chem. Res.* **1989**, *22*, 256.

(10) Belin, C.; Tillard-Charbonnel, M. *Prog. Solid State Chem.* **1993**, *22*, 59 and references therein.

0002-7863/93/1515-9089$04.00/0

Powder patterns were obtained from ground samples mounted between pieces of cellophane tape. An Enraf-Nonius Guinier camera, Cu Kα radiation (λ = 1.540 562 Å), and NBS (NIST) silicon as an internal standard were employed for this purpose. X-ray powder patterns calculated on the basis of the refined positional parameters for Z = Ni (below) matched the respective ones for the K–In–Pd and K–In–Pt products very well, leading to the conclusion that the same structure pertains to all three. A least-squares refinement of the measured and indexed 2θ values calibrated with standard Si lines resulted in a = 15.948(6) Å, b = 32.565(6) Å, c = 18.822(3) Å, V = 9775(7) Å^3 for $K_{10}In_{10}Ni$, a = 16.043(6) Å, b = 32.73(1) Å, c = 18.895(5) Å, V = 9921(5) Å^3 for $K_{10}In_{10}Pd$, and a = 16.056(3) Å, b = 32.692(5) Å, c = 18.896(3) Å, V = 9918(3) Å^3 for $K_{10}In_{10}Pt$. All of the patterns contained weak lines for indium metal as well, probably from adventitious oxidation of the very sensitive samples during the X-ray exposure.

A few crystals from the Ni product were sealed in glass capillaries and checked for singularity by oscillation film techniques. A zero-layer Weissenberg photograph of one 0.15 × 0.15 × 0.20-mm example revealed an *mmm* Laue class. Two octants of data up to 2θ = 50° (18 435 reflections) were collected from it at 23 °C with monochromated Mo Kα radiation on a CAD4 single-crystal diffractometer with ω–θ scans. Subsequent processing of the data and the structure refinement were done with the aid of the TEXSAN package.[11] Correction for Lorentz and polarization effects and for absorption (μ = 86.7 cm^{-1}) with the aid of the average of three ψ-scans at different 2θ angles gave a data set that showed systematic absences ($0kl$: $k+l \neq 2n$ and $hk0$: $h \neq 2n$) consistent with two possible space groups—*Pn2$_1$a* (No. 33) and *Pnma* (No. 62). Since the Wilson plot statistics indicated the existence of a center of symmetry, *Pnma* was chosen for the structure solution.

Application of direct methods (SHELXS-86[12]) provided 17 peaks with distances between them suitable for In and two smaller peaks with shorter distances to In than the others which were assigned to Ni. There were also eleven peaks with heights and distances suitable for K, but they were not assigned for the first few cycles. Successive least-square cycles and a difference Fourier synthesis revealed all 17 potassium positions. Refinement of all atoms with anisotropic thermal parameters and a secondary extinction coefficient gave final residuals of R, R_w = 2.9, 3.3% (4634 reflections $I > 3\sigma_I$, 299 variables). Occupancies of In or Ni did not deviate from unity by more than 1.0% (2.5σ) when the cations were held fixed, or those of K by more than 3.6% (4σ) when the In and Ni occupancies were kept fixed. All atoms were therefore retained at full occupancies for the final cycles. The remaining peaks in a final difference Fourier map were 1.4 e/Å^3, 1.07 Å from In5B, and −1.1 e/Å^3. Structure factor data are available from J.D.C.

The magnetizations of ~25-mg ground samples of single-phase samples of all three $K_{10}In_{10}Z$ phases were measured at a field of 3 T over 6–295 K and also at 100 Oe over 1.4–6 K on a Quantum Design MRMS SQUID magnetometer. The holder used for the purpose and the techniques are described elsewhere.[6]

Extended-Hückel calculations were carried out as before.[4-6,13] The H_{ii} values used for Ni and In in all three calculations were iterated to charge consistency and resulted in −6.4 and −2.33 eV for In 5s and 5p, respectively, and −7.38, −6.19, and −2.35 eV for Ni 3d, 4s, and 4p, respectively.[14] The charge iterations were done with the observed cluster plus 10 dummy potassium atoms placed far from the cluster and with the same symmetry. The H_{ii} values and s orbitals used for the potassium atoms were such as to ensure complete charge transfer to, and no significant overlap with, the cluster.

Results and Discussion

Structure Description. A general view of the unit cell for $K_{10}In_{10}Ni$ approximately along the c axis is shown in Figure 1 with connections drawn between all indium atoms that are less than 4.00 Å apart. Important near-neighbor distances are listed in Table I.

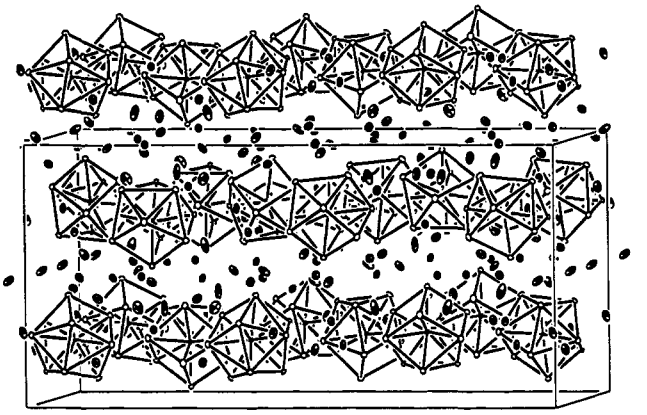

Figure 1. A general view of the unit cell of $K_{10}In_{10}Ni$ approximately along the 18.8 Å c axis. The well-separated Ni-centered clusters of 10 indium atoms (open ellipsoids) form close-packed layers stacked in hexagonal sequence along the a axis (vertical). The potassium cations (dark ellipsoids) separate both the layers and the clusters within each layer. Mirror planes lie at b = 1/4, 3/4. (20% probability ellipsoids).

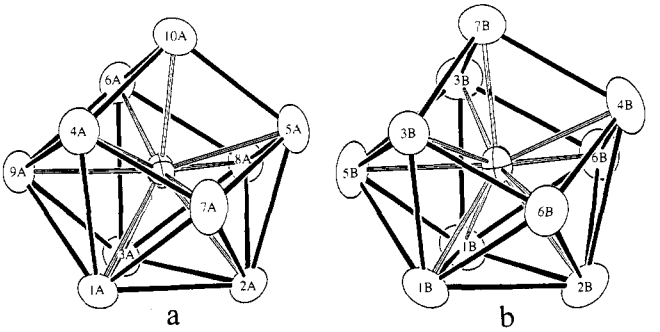

Figure 2. The independent Ni-centered clusters in $K_{10}In_{10}Ni$: (a) type A, with no symmetry; (b) type B with In2B, 4B, 7B, 5B, and Ni(B) on a mirror plane (94% ellipsoids).

The structure contains isolated 10-atom indium clusters that are centered by nickel and ordered in close-packed layers perpendicular to the a axis (vertical in Figure 1). Although all clusters are $In_{10}Ni$, they are of two crystallographically different versions (below), eight clusters of type A (centered by Ni(A)) and four of type B (centered by Ni(B)) per cell. Each cluster has six neighbors in the same layer as required for a close-packed layer, three of each type about the A-type clusters and six A-type neighbors about each B-type cluster. The layers are not quite flat but puckered along $\vec{a}$ by ~0.5 Å. The layers are stacked in a hexagonal packing order, which leads to quite large trigonal antiprismatic (ideally octahedral) voids between the layers.

The two indium clusters shown in Figure 2 have very similar geometries although different symmetries. Atoms in the cluster about Ni(A) lie on general positions, while In2B, In4B, In7B, In5B, and the central Ni(B) atoms lie on a mirror plane that gives the cluster C_s symmetry, Figure 2b. Both can be considered as derived from trigonal prism capped on all three rectangular and one triangular faces (C_{3v}). The former prisms, now distorted, are defined by In1A to 6A and In1B to 4B, while In7A–9A and InB5 and B6 cap the former rectangular faces of the prisms. Finally, In10A and In7B cap one expanded end face of each prism. All indium atoms have similar distances to the respective nickel atoms, which means the clusters must be substantially compressed along the quasi-3-fold axes through the axial In10A or 7B and the corresponding nickel atom. This in turn opens up the capped triangular face of the prism so that the edge distances are out of a reasonable bonding range, 4.19–4.53 Å. In order to keep the In–In distances around the cluster in a "normal" bonding range, the atoms capping the former rectangular faces [In(7–9)A, In(5,6)B] also move closer to the edges of the expanded

(11) TEXSAN, version 6.0 package, Molecular Structure Corp., The Woodlands, Texas, 1990.
(12) Sheldrick, G. M. SHELXS-86, Universität Göttingen, BRD, 1986.
(13) The orbital exponents used for In were from Janiak and Hoffman (Janiak, C.; Hoffman, R. *J. Am. Chem. Soc.* **1990**, *112*, 5924) and those for Ni were from Summerville and Hoffman (Summerville, R. H.; Hoffman, R. *J. Am. Chem. Soc.* **1976**, *98*, 7240).
(14) The parameters for charge iterations with one configuration for each orbital were from Munita and Letelier (Munita, R.; Letelier, J. R. *Theor. Chim. Acta* **1981**, *58*, 167) for In and from Mayers, Norman, and Loew (Mayers, C. E.; Norman, L. J.; Loew, L. M. *Inorg. Chem.* **1978**, *17*, 1581) for Ni.

Table I. Distances to Nearest Neighbors about Each Atom in $K_{10}In_{10}Ni$ ($d_{In-In} \leq 3.8$ Å, $d_{In-K} \leq 4.25$ Å, $d_{K-K} \leq 4.9$ Å)

In1A

In2A	3.158(1)	
In3A	3.120(1)	
In4A	3.354(1)	
In7A	3.160(1)	
In9A	3.096(2)	
NiA	2.784(2)	
K4	3.944(4)	
K4	3.709(4)	
K5	3.782(3)	
K8	3.666(4)	
K13	3.636(4)	

In2A

In1A	3.158(1)	
In3A	3.154(1)	
In5A	3.231(1)	
In7A	3.247(1)	
In8A	3.126(2)	
NiA	2.813(2)	
K4	3.794(4)	
K4	3.768(4)	
K7	3.682(3)	
K10	3.992(3)	
K11	4.035(3)	
K13	3.734(4)	

In3A

In1A	3.120(1)	
In2A	3.154(1)	
In6A	3.384(1)	
In8A	3.041(1)	
In9A	3.068(1)	
NiA	2.806(2)	
K1	3.678(3)	
K4	3.716(4)	
K10	3.836(3)	
K11	3.694(3)	
K12	3.768(4)	

In4A

In1A	3.354(1)	
In7A	2.968(1)	
In9A	2.949(1)	
In10A	2.968(1)	
NiA	2.754(2)	
K2	3.730(3)	
K3	4.038(4)	
K5	3.793(3)	
K8	4.135(4)	
K15	3.782(4)	
K16	4.039(5)	

In5A

In2A	3.231(1)	
In7A	3.020(1)	
In8A	2.972(1)	
In10A	2.931(1)	
NiA	2.745(2)	
K1	3.710(3)	
K7	4.101(4)	
K7	3.962(4)	
K11	3.761(3)	
K14	4.202(4)	
K17	3.740(4)	

In6A

In3A	3.384(1)	
In8A	2.958(1)	
In9A	2.959(1)	
In10A	3.029(1)	
NiA	2.697(2)	
K1	3.850(4)	
K3	3.488(3)	
K7	3.477(3)	
K12	3.747(4)	
K12	3.564(4)	

In7A

In1A	3.160(1)	
In2A	3.247(1)	
In4A	2.968(1)	
In5A	3.020(1)	
NiA	2.777(2)	
K7	3.499(3)	
K8	3.562(3)	
K15	4.130(2)	
K17	3.746(4)	

In8A

In2A	3.126(2)	
In3A	3.041(1)	
In5A	2.972(1)	
In6A	2.958(1)	
NiA	2.811(2)	
K7	3.573(3)	
K10	3.771(3)	
K11	3.518(3)	
K12	3.549(4)	
K13	4.010(4)	

In9A

In1A	3.096(2)	
In3A	3.068(1)	
In4A	2.949(1)	
In6A	2.959(1)	
NiA	2.816(2)	
K3	3.726(3)	
K5	3.692(3)	
K6	3.777(4)	
K11	3.605(3)	
K12	3.637(4)	

In10A

In4A	2.968(1)	
In5A	2.931(1)	
In6A	3.029(1)	
NiA	2.737(2)	
K3	3.763(3)	
K7	3.668(3)	
K14	3.738(4)	
K16	3.531(2)	

In1B

In1B	3.314(2)	
In2B	3.192(2)	
In3B	3.165(2)	
In5B	3.013(2)	
In6B	3.116(1)	
NiB	2.814(2)	
K6	3.638(4)	
K8	3.488(3)	
K9	3.489(4)	
K10	3.870(3)	

In2B

2 In1B	3.192(2)	
In4B	3.570(2)	
2 In6B	3.056(1)	
NiB	2.803(3)	
2 K8	3.637(4)	
2 K14	3.771(4)	
K15	4.221(8)	

In3B

In1B	3.165(1)	
In5B	3.060(1)	
In6B	2.992(1)	
In7B	2.937(1)	
NiB	2.785(2)	
K3	3.810(3)	
K5	3.630(3)	
K6	3.629(4)	
K9	4.073(4)	
K10	3.666(3)	

In4B

In2B	3.570(2)	
2 In6B	2.963(1)	
In7B	3.095(2)	
NiB	2.764(2)	
2 K3	3.721(3)	
2 K17	3.798(4)	

In5B

2 In1B	3.013(2)	
2 In3B	3.060(1)	
NiB	2.809(2)	
K2	3.659(5)	
2 K5	3.774(3)	
K9	3.453(5)	

In6B

In1B	3.116(1)	
In2B	3.056(1)	
In3B	2.992(1)	
In4B	2.963(1)	
NiB	2.763(1)	
K1	3.645(3)	
K3	3.896(4)	
K8	4.123(4)	
K10	3.769(3)	
K14	3.692(4)	

In7B

2 In3B	2.937(1)	
In4B	3.095(2)	
NiB	2.703(3)	
K2	3.817(5)	
2 K3	3.452(3)	
2 K6	4.027(4)	
K9	3.735(5)	

NiA

In1A	2.784(2)	
In2A	2.813(2)	
In3A	2.806(2)	
In4A	2.754(2)	
In5A	2.745(2)	
In6A	2.697(2)	
In7A	2.777(2)	
In8A	2.811(2)	
In9A	2.816(2)	
In10A	2.737(2)	

NiB

2 In1B	2.814(2)	
In2B	2.803(3)	
2 In3B	2.785(2)	
In4B	2.764(2)	
In5B	2.809(2)	
2 In6B	2.763(1)	
In7B	2.703(3)	

K1

In3A	3.678(3)	
In5A	3.710(3)	
In6A	3.850(4)	
In6B	3.645(3)	
K3	4.010(5)	
K4	4.483(5)	
K7	4.462(5)	
K10	4.243(4)	
K11	3.811(5)	
K12	4.046(5)	
K14	4.568(6)	
K17	4.017(5)	

K2

2 In4A	3.730(3)	
In5B	3.659(5)	
In7B	3.817(5)	
2 K3	4.401(5)	
2 K5	4.127(4)	
2 K6	4.165(5)	
K15	4.439(8)	
K16	4.016(8)	

K3

In4A	4.038(4)	
In6A	3.488(3)	
In9A	3.726(3)	
In10A	3.763(3)	
In3B	3.810(3)	
In4B	3.721(3)	
In6B	3.896(4)	
In7B	3.452(3)	
K1	4.010(5)	
K2	4.401(5)	
K6	3.913(5)	
K12	4.443(5)	
K16	3.995(7)	
K17	4.204(6)	

K4

In1A	3.944(4)	
In1A	3.709(4)	
In2A	3.794(4)	
In2A	3.768(4)	
In3A	3.716(4)	
K1	4.483(5)	
K4	3.858(7)	
K7	4.197(5)	
K8	4.134(5)	
K10	4.152(5)	
K11	4.889(5)	
K13	4.520(5)	
K13	4.043(5)	

K5

In1A	3.782(3)	
In4A	3.793(3)	
In9A	3.692(3)	
In3B	3.630(3)	
In5B	3.774(3)	
K2	4.127(4)	
K6	3.922(5)	
K6	4.835(5)	
K8	4.089(5)	
K9	4.289(5)	
K10	4.546(5)	
K11	4.783(5)	
K13	4.212(5)	

K6

In9A	3.777(4)	
In1B	3.638(4)	
In3B	3.629(4)	
In7B	4.027(4)	
K2	4.165(5)	
K3	3.913(5)	
K5	3.922(5)	
K5	4.835(5)	
K9	3.833(5)	
K10	4.824(5)	
K12	4.629(5)	
K13	4.714(6)	

K7

In2A	3.682(3)	
In5A	4.101(4)	
In5A	3.962(4)	
In6A	3.477(3)	
In7A	3.499(3)	
In8A	3.573(3)	
In10A	3.668(3)	
K1	4.462(5)	
K4	4.197(5)	
K11	4.829(5)	
K13	3.991(5)	
K14	4.131(6)	
K17	4.072(6)	

K8

In1A	3.666(4)	
In4A	4.135(4)	
In7A	3.562(3)	
In1B	3.488(3)	
In2B	3.637(4)	
In6B	4.123(4)	
K4	4.134(5)	
K5	4.089(5)	
K9	4.481(5)	
K10	4.674(5)	
K13	4.936(5)	
K14	4.075(6)	
K15	4.020(6)	

K9

2 In1B	3.489(4)	
2 In3B	4.073(4)	
In5B	3.453(5)	
In7B	3.735(5)	
2 K5	4.289(5)	
2 K6	3.833(5)	
2 K8	4.481(5)	

K10

In2A	3.992(3)	
In3A	3.836(3)	
In8A	3.771(3)	
In1B	3.870(3)	
In3B	3.666(3)	
In6B	3.769(3)	
K1	4.243(4)	
K4	4.152(5)	
K5	4.824(5)	
K8	4.674(5)	
K11	4.317(5)	
K12	4.265(6)	
K13	4.737(6)	

K11

In2A	4.035(3)	
In3A	3.694(3)	
In5A	3.761(3)	
In8A	3.518(3)	
In9A	3.605(3)	
K1	3.811(5)	
K4	4.889(5)	
K5	4.783(5)	
K7	4.829(5)	
K10	4.317(5)	
K12	4.190(6)	
K13	4.179(6)	
K13	4.695(6)	

K12

In3A	3.768(4)	
In6A	3.747(4)	
In6A	3.564(4)	
In8A	3.549(4)	
In9A	3.637(4)	
K1	4.046(5)	
K3	4.443(5)	
K6	4.629(5)	
K10	4.265(6)	
K11	4.190(6)	
K12	4.015(8)	
K13	4.401(5)	

K13

In1A	3.636(4)	
In2A	3.734(4)	
In8A	4.010(4)	
K4	4.520(5)	
K4	4.043(5)	
K5	4.212(5)	
K6	4.714(6)	
K7	3.991(5)	
K10	4.737(6)	
K11	4.179(6)	
K11	4.695(6)	
K12	4.401(5)	

K14

In5A	4.202(4)	
In10A	3.738(4)	
In2B	3.771(4)	
In6B	3.692(4)	
K1	4.568(6)	
K7	4.131(6)	
K8	4.075(6)	
K14	4.719(9)	
K15	4.774(7)	
K16	4.819(7)	
K17	4.202(8)	
K17	4.675(7)	

K15

2 In4A	3.782(4)	
2 In7A	4.130(2)	
In2B	4.221(8)	
K2	4.439(8)	
2 K8	4.020(6)	
2 K14	4.774(7)	
K16	4.340(9)	
2 K17	4.606(7)	

K16

2 In4A	4.039(5)	
2 In10A	3.531(2)	
K2	4.016(8)	
2 K3	3.995(7)	
2 K14	4.819(7)	
K15	4.340(9)	
2 K17	4.619(9)	

K17

In5A	3.740(4)	
In7A	3.746(4)	
In4B	3.798(4)	
K1	4.017(5)	
K3	4.204(6)	
K7	4.072(6)	
K14	4.202(8)	
K14	4.675(7)	
K15	4.606(7)	
K16	4.619(9)	
K17	4.502(8)	

triangular face. The foregoing cluster description seems much more useful than one based on pentagonal indium pyramids that are capped on the open face by a square (e.g., with In2A as the vertex and In(4,9,6,10)A as the square).

The $In_{10}Ni$ cluster geometries may be compared with those of the In_{11} and $In_{10}Hg$ clusters found in K_8In_{11} and $K_8In_{10}Hg$, respectively.[4,7] The latter are based on distorted pentacapped ($\sim D_{3h}$) rather than tetracapped trigonal prisms and do not have central atoms. The two axial atoms that cap the triangular faces of the trigonal prisms are shifted toward the center of the clusters to a much greater degree than in $In_{10}Ni$ so that the two expanded triangular faces have edge distances around 5 Å. In these cases, the compressions are sufficient to add bonding between the two types of face-capping atoms, at ~3.3 Å rather than 3.82–4.23 Å here (10A–7,8,9A, 7B–5,6B).

The Ni–In distances have a relatively small dispersion—from 2.697(2) to 2.816(2) Å and from 2.703(3) to 2.814(2) Å for the A and B types clusters, respectively, with an overall average of 2.78 Å. These distances compare reasonably well with the 9-fold Ni–In distance of 2.65 Å in more symmetric NiIn (CsCl-type)[15] and with the single bond radii sum for the two elements, 2.58 Å,[16] although the direct relationships among these are not so simple. The small dispersion means that the indium atoms are very close to the surface of an imaginary sphere around the central atom.

The In–In distances in the two Ni-centered clusters (Table I) are, in general, larger than commonly seen in other systems with bridged or isolated clusters, which are 2.85 to 3.1 Å, the shorter appearing particularly in two-center intercluster bonding.[4-8] Many of them here are in the 3.1–3.3 Å range and some are even greater than 3.3 Å. Apparently the size of the central element, the central bonding, and possibly the cation interactions (below) affect both the geometry of the cluster and the bonding between the In atoms. (The first variation is well-known in centered transition-metal halide clusters.[9]) The consequence of adding a central atom can be appreciated by a comparison of In–In distances in this cluster with those in the empty In_{11} since they have similar geometries and derivations. The average distances in the more-or-less vertical edges of the trigonal prisms, 3.323 and 3.300 Å here, are much greater than that that in In_{11}, 3.097 Å. The average distances in the uncapped triangular ends of the prisms of the Ni-centered clusters are also relatively long, 3.144 and 3.233 Å for the A- and B-types, respectively. A useful comparison can also be obtained with the In–In distances in $In_{10}Zn^{8-}$ ($\sim D_{4d}$).[8] The two clusters are isoelectronic and in fact differ only slightly in average In–In distances, 3.072 Å with Zn vs 3.090 and 3.094 Å for Ni, although the average Zn–In distance is somewhat greater than for Ni–In, 2.835 vs 2.777 Å. (Zn is also correspondingly 0.06 Å larger in metallic radius.[16]) This contrast appears to be a result of the different number of In–In bonds in the two cluster types. We find eight 3-bonded and two 4-bonded indium atoms in the Zn-centered cluster, but one 3-bonded, six 4-bonded, and three 5-bonded indium atoms in the Ni-centered clusters. The distances logically increase when there are more bonded neighbors, the five-bonded atoms in the latter having the more distant neighbors.

Cation Effects. It is not immediately clear, though, why the same two clusters (although isoelectronic) need to have different geometries and, therefore, differently bonded indium atoms. One possibility is that weaker (though shorter) Ni–In than Zn–In bonding may require more In–In bonds in the former to compensate for the lost central bonding. A more attractive explanation is simply packing requirements. We have repeatedly found that the ordering of the alkali-metal cations about faces, edges, and vertices of indium clusters in many structures is geometrically quite specific. The fact that there are two more cations per cluster in $K_{10}In_{10}Ni$ than in $K_8In_{10}Zn$ means that the former clusters will have more potassium neighbors. In order to accommodate them, the number and lengths of the In–In separations may have to be greater, meaning more edges and faces. More evidence regarding this can be found in bond populations (below).

Table II. Indium Neighbors of the Potassium Cations in $K_{10}In_{10}Ni$[a]

atom	CN[b]	N[c]	In atoms
K1	4	1	3,5,6A, 6B
K2	4	1	4,4A; 5,7B
K3	8	4	4,6,9,10A; 3,4,6,7B
K4	5	3 + 2	1,2,3A; 1,2A
K5	5	3 + 2	1,4,9A; 3,5B
K6	4	2 + 1	3,7B; 9A,1B
K7	7	4 + 3	5,7,8,10A; 2,5,7A
K8	6	3	1,4,7A; 1,2,6B
K9	6	4 + 2	3,3,5,7B; 1,1B
K10	6	3	2,3,8A; 1,3,6B
K11	5	3 + 2	2,5,8A; 3,9A
K12	5	3 + 2	3,6,8A; 6,9A
K13	3	1	1,2,8A
K14	3	2 + 1	2,6B; 10A
K15	4	2	4,7A
K16	4	2	4,10A
K17	3	2 + 1	5,7A; 4B

[a] $d < 4.2$ Å. [b] All K with 6 or more In neighbors have two d(K–In) values >3.85 Å within the set listed. [c] The orders of indium groups that are bonded to each potassium: 1, vertex; 2, edge; 3, triangular face; 4, quadrilateral face. Multiplicities of each type can be deduced from the second and last columns.

The layers of clusters as well as clusters within each layer are separated by the potassium cations (Figure 1). Similar ordering of the cations is also present in K_8In_{11} and $K_8In_{10}Hg$.[4,7] The thermal parameters for all potassium atoms in $K_{10}In_{10}Ni$ are relatively large (B_{eq} = 3.5(1)–8.6(4) Å^2) compared with those in the previous two and in $K_8In_{10}Zn$ which all fell in the range 3.0–5.0 Å^2.[4,7,8] This must result from the larger number of cations per cluster here than for the others, meaning more potassium and fewer indium neighbors for each cation. This, in turn, leads to longer K–K distances, more space around each potassium, and, consequently, greater positional freedom. The potassium atoms are again arranged so that they cap faces, bridge edges, and bond exo at vertices of the indium clusters. The potassium functionalities summarized in Table II reveal some clear regularities and order to these that also relate to ellipsoid differences. Distances are of course also important, and these can be recovered from Table I. Suffice for note here is the fact that all cations with apparent coordination numbers above five have two relatively long K–In distances >3.85 Å (the others range down to 3.45 Å).

The first eleven potassium atoms have smaller thermal parameters, 3.5(1)–4.9(2) Å^2. On the other hand, the last four, which are only three or four coordinate, have B_{eq} values between 7.2 and 8.6 Å^2, and these are also more anisotropic than the rest. The large thermal parameters probably result from the fact that these four atoms fill larger trigonal antiprismatic voids between close-packed layers of indium clusters and, therefore, have each other for neighbors as well as fewer indium neighbors. The anisotropic displacement parameters for these atoms are also somewhat greater along a, the antiprismatic axis, because they either bridge In–In cluster edges that are parallel to each other or bridge an edge and cap a vertex that are nearly coplanar with the cation. Such nearly planar environments usually allow greater motion normal to the plane of the surrounding atoms. In addition, these four cations do not have any potassium neighbors along the direction of the larger thermal motion, while K13 (B_{eq} = 5.6 Å^2), which also has only three indium neighbors, has surrounding potassium atoms that present a quite isotropic environment.

Because of the large number of potassium atoms per cluster, the shortest intercluster distance, 5.744(2) Å between In3A and In6A, is also greater than the 5.26 and 5.58 Å between the clusters in K_8In_{11} and $K_8In_{10}Zn$, respectively. In other words, the clusters

(15) Ruhl, R. C.; Giessen, B. C.; Cohen, M.; Grant, N. J. *Mater. Sci. Eng.* **1967**, *2*, 314.
(16) Pauling, L. *The Nature of the Chemical Bond*; Cornell University Press: Ithaca, New York, 1960; p 400.

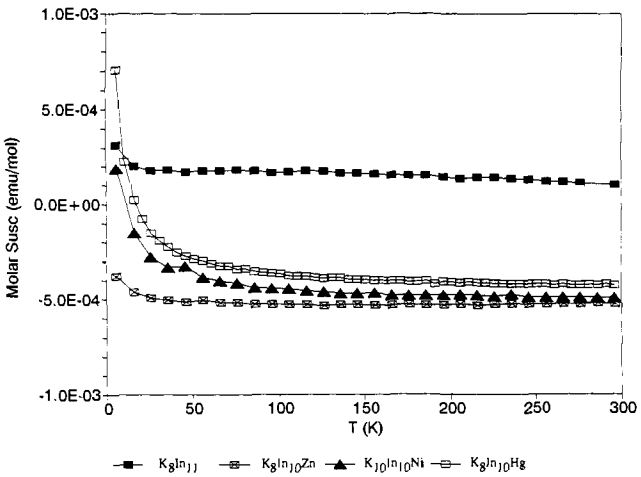

Figure 3. A plot of the molar magnetic susceptibilities of $K_{10}In_{10}Ni$ (filled triangles). Added for comparison are the susceptibilities of the diamagnetic $K_8In_{10}Hg$[7] (open squares) and $K_8In_{10}Zn$[8] (crossed squares) and of the Pauli-paramagnetic K_8In_{11}[4] (filled squares). All have received similar diamagnetic core and cluster skeletal electron corrections.

in $K_{10}In_{10}Ni$ are more loosely packed and more diluted by a sea of potassium cations than those other compounds. The distortions observed within the two clusters also suggest that these may be somewhat "soft".

Properties. The magnetic susceptibilities of the Ni, Pd, and Pt derivatives are temperature-independent over the range 25–295 K and, after holder corrections, fall in the range of $-(9–12) \times 10^{-4}$ emu mol^{-1}. There is no moment associated with Ni, Pd, or Pt, consistent with the bonding expectations (below). Two types of diamagnetic corrections can be applied to these numbers. The first, for the ion core diamagnetism, total −3.3, −3.5, and -3.6×10^{-4} emu mol^{-1} for the Ni, Pd, and Pt derivatives, respectively. A second correction, for the Larmor precession of the electron pairs in the large cluster orbitals, was calculated as before[4,8] with r_{ave} = 2.35 Å to yield $\chi_L = -3.0 \times 10^{-4}$ emu mol^{-1} for each compound. These give final χ_M values of $-(2.7–4.7)$, $-(4.5–5.5)$, and $-(4.5–5.5) \times 10^{-4}$ emu mol^{-1} over 25–295 K for Z = Ni, Pd, and Pt, respectively, clearly diamagnetic results. The susceptibility data for $K_{10}In_{10}Ni$ are shown in Figure 3 together with those similarly corrected for the diamagnetic $K_8In_{10}Hg$ and $K_8In_{10}Zn$ and the Pauli-paramagnetic K_8In_{11} ($8K^+ + In_{11}^{7-} + e^-$). No superconductivity was observed at low fields and at temperatures as low as 1.4 K. The crystal habits of these very reactive phases precluded gaining conductivity estimates by the Q-method that we have found useful in other cases. Resistances of the compounds were therefore checked by two-probe measurements on a few bar-like crystals with lengths of 3–5 mm. These yielded resistances of 2 to 4 kΩ ($\rho \sim 10^2$ Ω·cm), values that are 50–500 times those similarly measured for other poorly metallic or semimetallic indium cluster phases.[4-8] The high resistivities and the diamagnetic susceptibilities are in a good agreement with the crystal structure and the proposed electronic structure of the clusters (below).

Electronic Structure. Extended-Hückel MO calculations were performed on three different species: (a) an undistorted tetracapped trigonal prism (C_{3v}), (b) the empty C_{3v} symmetry cluster with the observed compression along the pseudo-3-fold axis, and (c) the foregoing cluster centered by Ni. All species had average distances equal to those observed. (Calculations with the geometries of the real clusters instead led to no more than 0.06-eV splitting of the degenerate orbitals and no significant differences between the A and B types.) The resulting MO energy diagrams are shown in Figure 4.

As expected, the ideal (but improbably proportioned) tetracapped trigonal prism has a closed shell with $2n$ electrons.[17] The top 10 orbitals (between −2.3 and −3.0 eV) below a small gap of

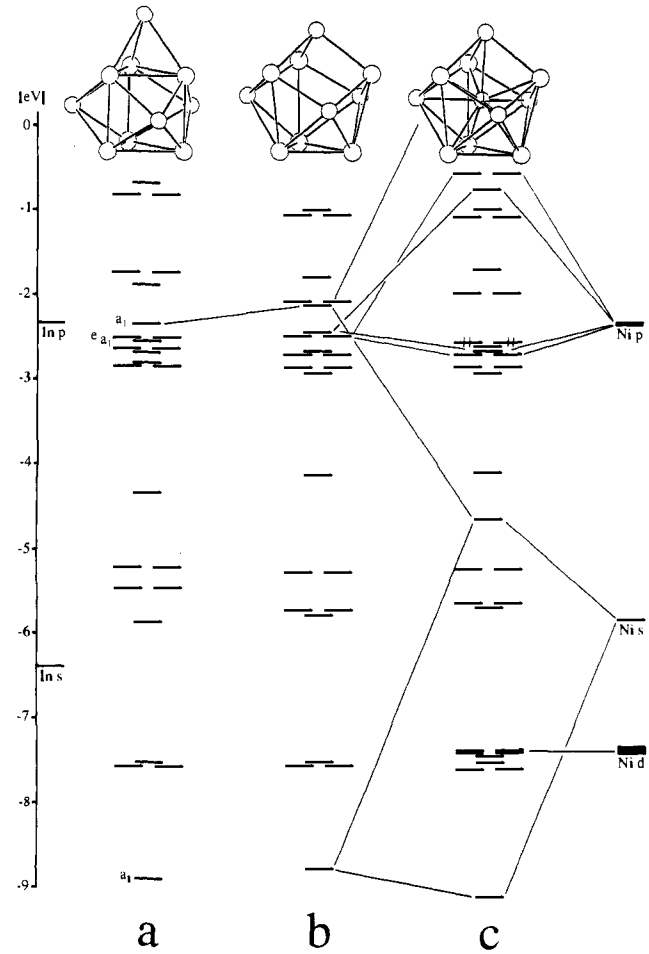

Figure 4. Charge-consistent EHMO results for $K_{10}In_{10}Ni$ (C_{3v}): (a) the undistorted tetracapped trigonal prism; (b) In_{11} distorted to the observed polyhedron; (c) as in $In_{10}Ni^{10-}$.

~0.5 eV (Figure 4a) are of mainly p character and carry the skeletal bonding electrons. A block of orbitals of mainly s-character spreads from −4.3 to −9.0 eV, combinations of the so-called lone pairs on the indium. (As before,[8] the HOMO for the s block near −4.3 eV exhibits significant hybridization of s and p.) Upon distortion to b, nothing significant happens to the s block, as it should be, and also to the lower 9 of 10 skeletal bonding orbitals. Those that do change are the a_1 HOMO and some of the antibonding levels. A closer look reveals that this a_1 is bonding within the triangular ends of the prism and antibonding between the unique capping atom and those in the capped triangle. The observed axial compression raises the a_1 energy on both accounts.

Orbitals with similar behaviors are also found in the pentacapped trigonal prism of In_{11} and the bicapped square antiprism of $In_{10}Zn$ when these are axially compressed. The a_1 orbital in the former is destabilized to a greater degree (by 2 eV) because the atoms capping the triangular faces of the prism are pushed much closer to the center of the cluster (above) and both triangular ends are capped. In the Zn-centered cluster, the change in the energy of the a_1 orbital at this stage is about the same as that with the Ni-centered example because, first, the compression of the cluster is not as pronounced as in the pentacapped trigonal prism simply because it is limited by the central atom, and second, the destabilization is not as large since the larger squares need not expand as much in order to accommodate the compression and more π antibonding components are already present. As an

(17) A tricapped trigonal prism (9 atoms), a regular *closo* deltahedron, requires $2n + 2 = 20$ electrons according to Wade's rules. Addition of an In^+ cation along the 3-fold axis generates no new orbitals. The skeletal electron count thus remains at 20 which is now $2n$.

example, the edges within the squares increase to 3.625 Å while those in the triangles of the pentacapped trigonal prisms go to 5.00 Å. (Some of the antibonding orbitals fall in energy during compression (Figure 4b) because they are in character opposite to that of a_1, antibonding within the triangles of the prism and bonding between the capping atom and the triangle.)

Introduction of the Ni atom at the center of the cluster produces a very interesting result (Figure 4c). The Ni d orbitals remain unperturbed as they exhibit negligible mixing with cluster orbitals. In effect, this appears to come about because of the appreciable difference between the energies of the skeletal cluster orbitals around −2.5 eV and of the Ni d orbitals located around −7.5 eV; in other words, the nickel is fully reduced and d^{10}. The resulting In–Ni distances are thus too long for good overlap between Ni d and In s, p. A similar conclusion regarding inertness of the Ni d orbitals has been deduced for several Ni-centered nickel carbonyl clusters, $Ni_9(GeEt)_6(CO)_8$ (a body-centered cube capped on all faces by GeEt),[18] as well as in $[Ni_{11}(SbNi(CO)_3)_2CO)_{18}]^{2-}$ [19] and $[Ni_{11}(SnR)_2CO_{18}]^{2-}$,[20] centered icosahedra containing two trans Sb or Sn atoms and 2.057–2.58-Å Ni–Ni distances. The conclusion that there are no significant Ni–Ni bond populations for interstitial–cage distances above ~2.5 Å[20] translates into Ni–In distances ~2.77 Å on the basis of metallic radii, comparable to what are found here.

On the other hand, the Ni s and p orbitals are of appropriate energies and apparently appropriate sizes to overlap well with certain cluster molecular orbitals. The Ni s orbital mixes with two a_1 orbitals from the cluster. The upper one was the HOMO for the ideal tetracapped trigonal prism (Figure 4a) that was pushed higher during the distortion leading to the observed cluster geometry (Figure 4b), while the other cluster a_1 is the lowest orbital in the s-block. The charge distribution in the middle a_1 result is ~50% Ni s, 30% In p, while the radial orbital that is pushed up appreciably is about 80% In p. The Ni p orbitals, which tranform as a_1 and e for this point group, mix with appropriate combinations from the cluster (Figure 4c) to increase the HOMO–LUMO gap to ~0.5 eV. The net result of the insertion of the central element is the stabilization of some cluster orbitals and a gain of In bonding to the central Ni atom, although it is difficult to be more specific regarding the latter bond energies. The cluster has a closed shell with $2n = 20$ skeletal electrons and therefore a −10 charge, $In_{10}Ni^{10-}$. A comparable result was obtained from calculations on the Zn-centered $In_{10}Zn^{8-}$ with a geometry of a bicapped square antiprism. In that case, a Zn atom not only lowered the energies of some of the cluster orbitals but also provided two of the bonding electrons. The resulting cluster is isoelectronic with $In_{10}Ni^{10-}$, both having closed $3d^{10}$ cores on the interstitial atoms. The two are also isoelectronic with In_{11}^{7-} when In 5s states are included.

Comparison of the EHMO results with those for $In_{10}Zn^{8-}$ also provides some information regarding the different geometries of the indium shells and the increases in both In–In distances and the number of nearest neighbors about each vertex observed in the nickel case. Our assertion earlier was that the last appeared to be related to the larger number of cations to be accommodated. The calculated In–In bond populations average 0.826 per vertex in $In_{10}Ni^{10-}$ vs 0.761 in $In_{10}Zn^{8-}$, i.e., there is greater bonding in the In shell that is "solvated" by the greater number of cations. The Ni–In populations are 2.23 while those for Zn–In (with an intrinsically different overlap) total 2.32. The latter separations are longer, in amount appropriate to the single bond radii differences.

We also note that $In_{10}Ni^{10-}$ can be readily related to Sb_7^{3-} electronically and geometrically which is a *monocapped* trigonal prism.[21] Removal of the three nonbonding electron pairs on the two-bonded antimony atoms (compare P_4S_3) corresponds to the (hypothetical) indium fragment In_7^{11-}. This in turn translates to $In_{10}Ni^{10-}$ when (a) the three trapezoidal faces of the M_7 species are capped by In^+, (b) the polyhedron is centered by d^{10} Ni(0), and (c) one electron pair is added. The last is necessary to fill the newly developed a_1 radial orbital in the 11-atom closed polyhedron.

The apparent inertness of the d orbitals on the central Ni, Pd, and Pt atoms in these indium clusters may be behind our failure to synthesize clusters centered by earlier transition metals with fewer d electrons. If orbitals on at least the immediately preceding interstitials are again low in energy, electron transfer from the well-reduced indium cluster to the d shell should again fill it to d^{10}. This circumstance may well be unfavorable since an earlier Z element would require an even greater cation content and negative charge on the cluster. On the other hand, the valence p on these candidates may also become too high for good bonding. In matter of fact, attention to aspects of bonding only in potential analogues with different Z is far too one-sided; any question of stability in equilibrium systems must also address the stabilities of all *alternate* products, and these may vary significantly with Z.

Phases with the $K_{10}In_{10}Z$ type structure and clusters reported here appear to have some broader occurrence and wider importance. First, we have recently discovered that the isostructural $Na_{10}Ga_{10}Z$ can be synthesized directly. A related copper phase ~$K_{10}In_{10}Cu$ gives a very similar powder pattern, but it unfortunately has a superlattice with one dimension >~70 Å. Refinement of the subcell cell to $R \sim 15\%$ shows three similar clusters, one partially disordered, but all of the cations cannot be located. The same or closely related $Na_{10}In_{10}Z$ phases also appear in the respective systems according to powder patterns although single crystals all appear to be twinned.[22] More significantly, these sodium phases are formed in the presence of large amounts of the very novel $Na_{96}In_{97}Z_2$ which contain condensed, fullerene-like $Na_{39}In_{74}$ and other units in shells. These and other condensed macroclusters in $Na_{172}In_{197}Z_2$ are all centered by somewhat disordered versions of the same or closely related $In_{10}Z^{10-}$ clusters.[22,23]

Acknowledgment. Victor Young and Jerome Ostenson were helpful with the diffractometer and susceptibility studies.

Supplementary Material Available: Tables of data collection and refinement information, positional and anisotropic displacement parameters for 36 atoms, and an illustration of cluster packing systematics in $K_{10}In_{10}Ni$ (4 pages). Ordering information is given on any current masthead page.

(18) Zebrowski, J. P.; Hayashi R. K.; Bjarnason, A.; Dahl, L. F. *J. Am. Chem. Soc.* **1992**, *114*, 3121.
(19) Albano, V. G.; Demartin, F.; Iapalucci, M. C.; Longoni, G.; Sironi, A.; Zanotti, V. *J. Chem. Soc., Chem. Commun.* **1990**, 547.
(20) Zebrowski, J. P.; Hayashi, R. K.; Dahl, L. F. *J. Am. Chem. Soc.* **1993**, *115*, 1142. Dahl, L. F., private communication, 1992.
(21) Adolphson, D. G.; Corbett, J. D.; Merryman, D. J. *J. Am. Chem. Soc.* **1976**, *98*, 7234.
(22) Sevov, S. C.; Henning, R. W.; Corbett, J. D., unpublished research.
(23) Sevov, S. C.; Corbett, J. D. *Science*, accepted for publication.